Springer

KSME

Journal of Mechanical Science and Technology 31 (3) (2017) 1365~1372
www.springerlink.com/content/1738-494x(Print)/1976-3824(Online)
DOI 10.1007/s12206-017-0236-8

On performance studies during micromachining of quartz glass using electrochemical discharge machining †

Mudimallana Goud and Apurbba Kumar Sharma*

Indian Institute of Technology Roorkee, Roorkee, 247 667, India

(Manuscript Received March 17, 2016; Revised November 8, 2016; Accepted November 18, 2016)

Abstract

The electrochemical discharge machining is a highly stochastic process involving a number of complex parameters. Controlling of these process parameters simultaneously to fetch the best possible performance is a difficult task. Determining an optimal parametric combination has become complex owing to interdependency of the parameters. In this work, the authors have made an attempt to establish the optimal combination of control parameters for machining of micro-channels on quartz glass. Taguchi's standard orthogonal array (L_9) with Grey relational analysis (GRA) approach was used to establish the optimal parametric conditions for reducing the Width overcut (WOC) of micro-channels and increasing the Material removal rate (MRR). In order to optimize MRR and WOC together, the optimal combination of the selected control variables was obtained using the GRA. The experimental results showed the effectiveness of the adapted method to indicate the performance of the electrochemical discharge machining process.

Keywords: Quartz glass; ECDM; MRR; WOC; GRG; Electrolyte; ANOVA

1. Introduction

The Electrochemical discharge machining (ECDM) has high potential to be used for machining non-conducting materials, such as glass. In Microelectromechanical systems (MEMS), the importance of glass is growing due to its useful properties such as scratch resistance and chemical inertness. However, glass offers considerable processing challenges in terms of methods and cost effectiveness. And various techniques have been explored to machine glass so as to compete on price and performance without compromising on profitability. Processes like ultrasonic machining have proved effective in the micro domain; however, the performance of the process and tool design remains as the major concern.

Investigation in the machining of glass using ECDM has been on the rise in the recent years. Micro-structuring of glass by ECDM was reported by several researchers. Bhuyan and Yadava [1] have applied the Taguchi method coupled with Weighted principal component (WPC) for modelling and then Taguchi method coupled with Response surface methodology (RSM) for optimizing the Traveling wire Electro-chemical spark machining (TW-ECSM) process. In first stage they found the optimum parameters level and in the next stage second-order response model was developed using RSM for optimizing the surface roughness and material removal rate. Chang et al. [2] have drilled micro-holes in Pyrex glass with a cylindrical tool of 200 μm diameter at different applied voltages (40 and 45 V). Zheng et al. [3] reported fabrication of 3D structures on the pyrex glass using layer-by-layer approach with pulsed voltage. The grooves were fabricated using a feed rate of 1000 μm/min per stroke and 50 μm as working depth for each layer until the required depth was reached. Goud et al. [4] reviewed the material removal mechanism concept and identified the scopes for further research. They suggested some possible efforts to enhance the MRR in ECDM such as providing continuous supply of optimum amount of electrolyte to the machining zone, using rotating tool-electrodes that can avoid the discharge focused on the same point, maintaining machining gap between tool-electrode and the workpiece, appropriate tool motion in abrasive mixed electrolyte. Han et al. [5] reported fabrication of contour on soda-lime glass with a surface-textured tool. Cao et al. [6] had machined micro-channels of size 30 μm depth, 1000 μm length and 40 μm width on pyrex glass; they also reported fabrication of micro pillars (55 μm of height) and micro-walls (10 μm thickness) on soda lime glass.

Jung and Kwon [7] have used the grey relational analysis theory to overcome the limitation of Taguchi design as the Taguchi method was designed only to optimize the single response characteristic. They attempted to find the optimal process parameters combination to machine the minimum

*Corresponding author. Tel.: +91 1332 285421, Fax.: +91 1332 273560
E-mail address: akshafme@iitr.ac.in
† Recommended by Associate Editor Jongbaeg Kim

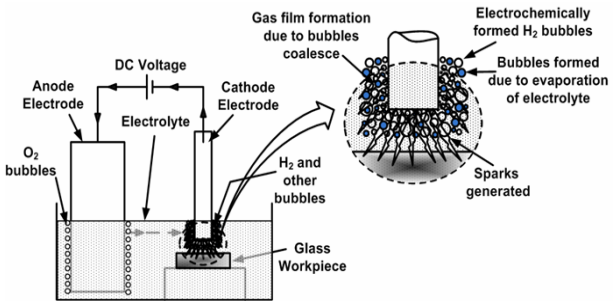

Fig. 1. Principles of electrochemical discharge machining.

diameter micro-hole with a maximum aspect ratio using electrical discharge machining process. Adalarasan et al. [8] have found the optimal process parameters combination for individual response parameters using Taguchi's L_9 orthogonal array, and then they applied grey relational analysis to find optimal setting of process parameters for friction welding to investigate the bond strength and hardness of the friction welded joints. Kim [9] has applied a Taguchi's orthogonal array of L_{18} to identify the optimum set of the control factors for minimizing the noise of operation of an indoor Package air-conditioner (PAC). The author had found the improvement in sound performance of PAC by 3.71 % dBA, and a reduction of about 8.37 % RPM in number of revolutions of the fan. Lijo and Hiremath [10] studied the effect of various control parameters to machine desired micro-channels on soda lime glass. They have conducted experiments using Design of experiment (DOE) approach and response surface modelling was used for characterization of response parameters surface finish and MRR. Jawalkar et al. [11] studied micromachining of soda lime glass using NaOH and $NaNO_3$ electrolytes. They applied the Taguchi's L_9 orthogonal array to study the parametric effect on Material removal (MR). Their results revealed that applied voltage was the most dominating parameter followed by electrolyte concentration and distance between the electrodes. Gupta et al. [12] presented a comprehensive review on the effect of tool-electrode process parameters like tool geometry, tool motion, wettability, insulation, feed, temperature and concentration of electrolyte which have shown improvement in accuracy and efficiency in the ECDM process. Study on MRR of pyrex glass by Yang et al. [13] showed that maximum MRR would be achieved is 0.7 mm^3/min with KOH electrolyte added with SiC abrasives while the tool-electrode was of brass material. Cao et al. [14] reported maximum MRR of 200 μm^3/s while machining soda lime glass with KOH electrolyte and tungsten carbide tool. Feng and Hua [15] proposed an optimization method for precision forging of helical gears based on finite element method and Taguchi method. The optimal process parameters combination was obtained by S/N ratio analysis for the response parameters forging force and die-fill quality. They observed deformation temperature was the most significant parameter followed by friction coefficient and punch velocity.

The relevant literatures thus indicate that significant work have been reported on parametric influence on the process responses. There is hardly any investigation on process performance in terms of WOC and MRR. The WOC is a significant response parameter, especially in the micro machining domain. The MRR, although not an important on the accuracy indicator parameter, could prove meaningful in high volume production on scale of economy. The present work addresses the performance analysis of the ECDM process considering both MRR and WOC as the response parameters.

2. Working principles of ECDM

Fig. 1 shows a schematic diagram depicting the working principle of the ECDM process. In the usual configuration, the workpiece is kept dipped in an electrolyte (KOH, NaOH, $NaNO_3$ based etc.). The tool-electrode tip is immersed one to two millimeters in the electrolyte and a large counter electrode is kept a few centimeters away from the tool-electrode. The submerged surface area of the tool-electrode should be significantly smaller (usually, by a factor of about 1/100) than the counter-electrode submerged surface area. In general, the tool-electrode is polarized as cathode and the counter-electrode as anode (direct polarity). A DC or a pulsed voltage is applied between the electrodes. At an applied voltage, typically around 25 V (lower than a critical voltage), electrolysis occurs and consequently, generation of oxygen bubbles results at the auxiliary (counter) electrode and hydrogen bubbles at the tool-electrode. The electrochemical reactions are as below:

$$2H_2O + 2e^- \rightarrow 2(OH)^- + H_2 \uparrow \quad \text{(at Cathode)}$$
$$4(OH)^- \rightarrow 2H_2O + O_2 \uparrow + 4e^- \quad \text{(at Anode).}$$

The density of the bubbles and their size can be increased by increasing the current density. As the applied voltage crosses the critical value, the coalescence of the hydrogen bubbles starts at the cathode that results in formation of a gas film around the tool-electrode as shown in the enlarged view of the machining zone. The gas film acts as a dielectric resistance and creates a high potential difference between the electrodes. As the potential difference becomes high enough for a given pair of tool-electrolyte system, electrical discharges (in the form of light emission) do occur between the electrolyte and the tool-electrode, also called as the discharge zone. If the workpiece is placed in the discharge zone, machining of the material proximity to the zone does take place in the form of melting, vaporization and thermal erosion due to the heat of discharges. If the discharge condition is maintained, and the workpiece is fed at a regular speed to compensate for the eroded material in the discharge zone, an electro-thermal based machining configuration is obtained. Further, simultaneous chemical etching of work material also contributes to the machining operation, although significantly less. In this process, the selection of the parameters to maintain the favorable conditions for continuous discharge is tricky and obtaining an optimal combination of the parameters to achieve usu-

Table 1. Major properties of quartz glass.

Density	0.0022 g/mm^3
Young's modulus	7.25 × 10^4 N/mm^2
Softening point	1683 °C (Approximately)
Poisson's ratio	0.17

Table 2. Experimental conditions.

Constant parameters	
Auxiliary electrode material	Graphite
Tool-electrode material	Stainless steel (Ø 0.45 mm)
Workpiece material	Quartz glass
Electrolyte	NaOH
Level of electrolyte	Approx. 01 mm above the workpiece
Gap between the top surface of work-piece and the tool-electrode	Around 25 µm
Inter-electrode gap	50 mm
Machining time	3 min
Variable parameters	
Applied voltage	40-50 V
Electrolyte concentration	20-30 wt%
Feed rate	3-5 mm/min

ally conflicting objectives of high MRR and higher machining accuracy is challenging.

3. Experimental setup and control parameters

3.1 Experimental conditions and machining setup

Stainless steel tool-electrodes (0.45 mm diameter) were used in the present investigation. Quartz glass specimens of the square shape of size 20×20×2 mm (major properties are shown in Table 1) and NaOH were used as the workpiece and electrolyte, respectively, for the trials. The elemental composition of the quartz glass was assessed through Energy dispersive spectrometry (EDS); the corresponding spectrum confirms weight percentages of Silicon and Oxygen as 55.3 and 44.7, respectively. The machining time considered for the trials was three minutes. A full-wave rectified D.C. power supply was used as the energy source; other conditions chosen for experimentation are shown in Table 2. The process parameters and their levels were selected based on literature survey [3-6, 10, 11] and the results of preliminary experiments conducted considering the capabilities of the homebuilt setup and other resource constraints. The preliminary experiments were conducted for making micro-channels by varying the individual process parameter to study its effect on the response characteristics of the process (One-factor-at-a-time, OFAT). Machining of micro-channels was performed at the ambient temperature with electrolyte flow and stirring.

A 3-axes, stepper motor controlled ECDM setup, interfaced with a personal computer, was developed for the experimentation. Fig. 2(a) shows a 3D schematic view of the developed setup. The 3-axes of the setup (each axis is controlled by a separate stepper motor of 10 kg-cm torque), consists of a two-axes work table with relative movement between them. Further, a control unit comprising of a 24 V, 10 A DC power supply, parallel port buffered breakout board and 5 A micro-stepping drive for each axis was developed. The setup was interfaced with a computer and the axes of the setup were controlled by MACH3 software [16]. Fig. 2(b) shows the developed experimental setup.

Table 3. Process parameters and their levels.

Symbol	Process parameters	Level		
		1st	2nd	3rd
A	Applied voltage (V)	40	45	50
B	Electrolyte concentration (wt%)	20	25	30
C	Feed rate (mm/min)	3	4	5

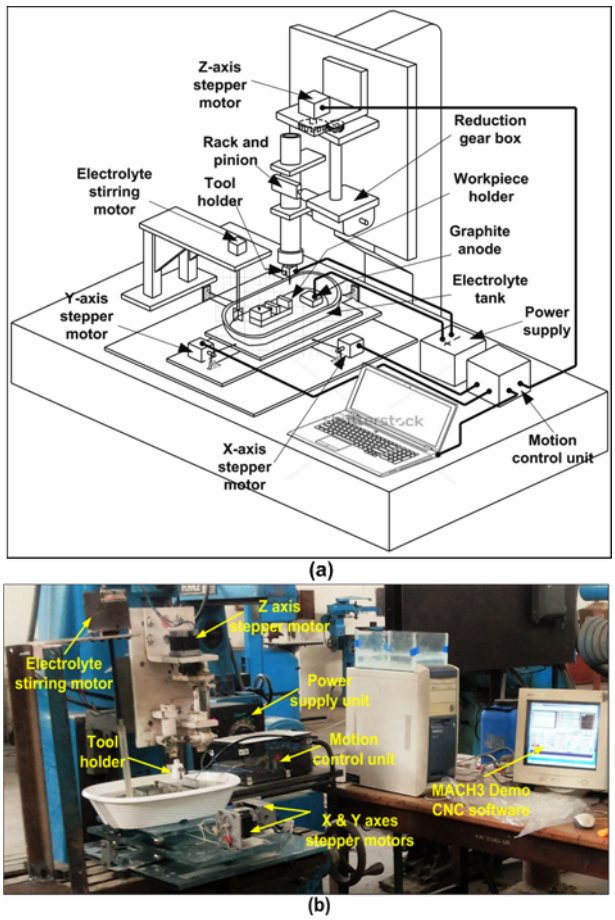

Fig. 2. ECDM experimental setup: (a) Schematic diagram; (b) photograph.

The initial control parameters were: applied voltage (40 V), concentration of electrolyte (20 wt%) and feed rate (3 mm/min). The ranges of machining parameters were obtained after performing the basic experiments using initial machining parameters. Accordingly, the feasible range of applied voltage

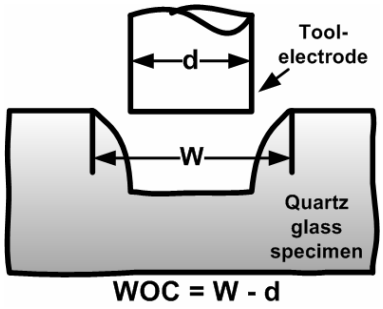

Fig. 3. Schematic diagram of assessment of WOC.

was 40-50 V, the electrolyte concentration range 20-30 wt% and the feed rate range 3-5 mm/min. In the present investigation, each control parameter at three levels were selected (Table 3) based on the setup capabilities and the domain data in the literature.

3.2 Measurement of machining performance

In this investigation, two parameters MRR and WOC were taken as the response parameters or performance criteria. The experimentation was carried as per the standard orthogonal array (L_9) design and the responses were measured after each experimental run. The MRR was measured as $\{(w_1 - w_2)/(\rho \times t)\}$ where w_1 and w_2 are the weights (g) of the quartz glass specimen before machining and after machining, respectively, t is the machining time (min) and ρ is the density of the workpiece (g/mm^3). The WOC was computed as $(W - d)$, where W is the machined channel width (mm) and d is the tool-electrode diameter (mm) (Fig. 3). The widths of the channels were measured using a stereomicroscope (model: SMZ745T, make: NIKON) and the specimen weights (before and after machining) were measured on a digital weighing machine (model: AUW220 D, make: SHIMADZU, least count: 0.01 mg); an average of three measurements were considered.

4. Experimental design

The experimentation was carried as per Taguchi's standard orthogonal array L_9 (3^3-three factors at three levels) to find out the optimal parametric combination for the machining. In the present investigation, three control parameters were used and the interaction between them was neglected. In case of three parameters at three levels, the total Degrees of freedom (DOF) are 7 [= 1+ (3 × (3-1))] which suggest that to analyze the effect of each parameter at least seven experiments are to be conducted.

The experimental design for three variables with corresponding experimentally obtained mean values of MRR and WOC are presented in Table 4. The optimal combinations of the machining parameters were obtained and verified using the analytical study of signal-to-noise ratio and ANOVA. In this present investigation, 'smaller-the-better' and 'larger-the-better' quality characteristics were used for WOC and MRR, respectively for obvious reasons.

Table 4. Experimental design and mean values of MRR and WOC with their respective S/N ratios and performance index ratios.

Trial no.	Control parameters			Response parameters		S/N ratios	
	Applied voltage (V)	Electrolyte concentration (wt%)	Feed rate (mm/min)	Average MRR (mm^3/min)	Average WOC (mm)	MRR (dB)	WOC (dB)
1	40	20	3	0.1515	0.0545	-16.391	25.271
2	40	25	4	0.3697	0.0874	-8.643	21.167
3	40	30	5	0.5556	0.1076	-5.106	19.367
4	45	20	4	0.3051	0.0603	-10.313	24.396
5	45	25	5	0.5278	0.1774	-5.551	15.022
6	45	30	3	0.4591	0.2537	-6.762	11.915
7	50	20	5	0.5530	0.1957	-5.145	14.169
8	50	25	3	0.4621	0.2418	-6.705	12.330
9	50	30	4	0.5919	0.3654	-4.555	8.744

The values of S/N ratios for MRR and WOC, calculated using well established mathematical formulae [8, 9] are shown in Table 4. Accordingly, the trial condition at trial no. 9 would indicate the best process performance corresponding to the (-ve) smallest S/N ratio amongst the MRR values.

5. Results and discussions

5.1 Analysis of S/N ratio

The plots of S/N ratio are useful to determine the optimal control parameter. Generally, a control parameter corresponding to the higher S/N ratio is considered as the dominant that could affect the experimental results significantly. In this study, a delta value (difference between the highest and the lowest mean S/N ratio) was used to find out the optimum process parameter. The values of delta for all the three control parameters are presented in Table 5.

It is observed from the delta values for MRR and WOC (Table 5) that the MRR was significantly influenced by electrolyte concentration (highest: 5.142), followed by feed rate, and applied voltage (lowest: 4.578). Accordingly, the parameters may be ranked as shown in the Table 5.

On the other hand, the WOC was highly influenced by applied voltage (highest: 10.187), followed by the concentration of electrolyte, and then the feed rate (lowest: 1.917) and were ranked 1, 2 and 3, respectively. Figs. 4(a) and (b) show the graphical representation of MRR and WOC mean S/N ratios, respectively for all the control parameters. Fig. 4(a) shows that the optimal parametric combination for maximized MRR was A3B3C3, i.e., applied voltage: 50 V, concentration of electrolyte: 30 wt% and feed rate: 5 mm/min. The mean S/N ratio graph of MRR (Fig. 4(a)) reveals that at higher levels of all the three parameters the MRR is maximum owing to the fact that the high applied voltage generates high intensity sparks at

Table 5. Mean S/N ratios and delta values for the response parameters.

Level	MRR's mean S/N ratio			WOC's mean S/N ratio		
	Voltage	Electrolyte concentration	Feed rate	Voltage	Electrolyte concentration	Feed rate
1	-10.046	-10.616	-09.952	21.935	21.278	16.505
2	-07.542	-06.966	-07.836	17.111	16.172	18.102
3	-05.468	-05.474	-05.267	11.747	13.342	16.186
Delta	04.578	05.142	04.685	10.187	07.936	01.917
Rank	3	1	2	1	2	3

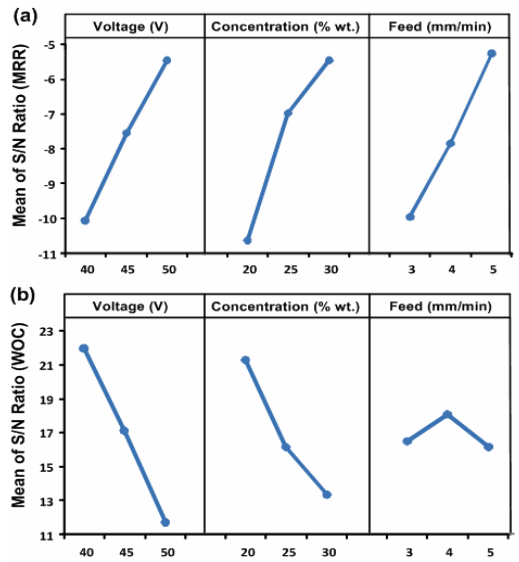

Fig. 4. Mean S/N ratio plots for (a) MRR; (b) WOC.

high frequency. Higher level of concentration of electrolyte expedites the rate of gas bubble generation, which in turn increases the discharge frequency due to rapid film formation around the electrode; it also enhances chemical etching. Further, higher feed rate exposes more nascent work material to the sparking zone causing more material to get ablated. The combined effect, thus, leads to an overall increase in MRR. The graphs of WOC with respect to mean S/N ratio (Fig. 4(b)), on the other hand shows the optimal parameter combination for the minimum WOC as A1B1C2, i.e., applied voltage: 40 V, concentration of electrolyte: 20 wt% and feed rate: 4 mm/min. The reason for minimum WOC can be explained by the fact that the low intensity of sparks are generated (also at low frequency) at lower levels of applied voltage, less amount of chemical etching at lower concentration of electrolyte. However, the variation of WOC due to change in feed rate shows a different trend (ascending from level 1 to level 2 and then descending from level 2 to level 3) compared to the applied voltage and electrolyte concentration. The reason for this varying trend can be explained by the fact that at the lower feed rate the time of contact between the work specimen and the sparks would be sufficient to heat and melt the workpiece quickly that results in higher overcut. This effect of higher overcut decreases as the feed rate increases and the time of contact between workpiece and sparks uniformly reduces up to level two feed rate approximately; beyond this, again the trend changes the direction possibly due to increase in electrolyte temperature that enhances the chemical etching of the work material. Therefore, in this case, it is not possible to identify the most significant (common for both MRR and WOC) control parameters level for the ECDM process as both the response parameters MRR and WOC get influenced in a different fashion by different parametric combinations.

5.2 GRA for multi-objective optimization

To overcome the limitations of S/N ratio analysis as discussed in the previous section, the Taguchi method with GRA is widely used [10, 11, 17, 18]; the approach is useful for solving and analyzing problems of multi-objective optimization. In GRA, the problem of multi-objective optimization is converted into a problem of single-objective optimization to determine the optimal control parameter combination that results in desired quality characteristics (response characteristics).

In the present investigation, as there are two response parameters of different objectives, which are 'higher-the-better' (MRR) and 'lower-the-better' (WOC), the different normalization methods were used. Both were of linear and normalized in the range between zero and one.

Accordingly, for MRR and WOC, normalization was carried out using Eqs. (1) and (2), respectively.

$$\left(y_i\right)_{mrr} = \frac{\left(x_i\right)_{mrr} - \min\left(x_i\right)_{mrr}}{\max\left(x_i\right)_{mrr} - \min\left(x_i\right)_{mrr}} \tag{1}$$

$$\left(y_i\right)_{woc} = \frac{\max\left(x_i\right)_{woc} - \left(x_i\right)_{woc}}{\max\left(x_i\right)_{woc} - \min\left(x_i\right)_{woc}} \tag{2}$$

where i is the number of the experiments, $\left(x_i\right)$ is the measured results, $\min\left(x_i\right)$ and $\max\left(x_i\right)$ are the minimum and maximum values of $\left(x_i\right)$, respectively. The normalized values of performance characteristics are shown in Table 6.

In this approach, Grey relational coefficients (GRC) were calculated using following relationships:

$$\xi_i^k = \frac{\Delta_{\min}^k + \lambda\Delta_{\max}^k}{\Delta_i^k + \lambda\Delta_{\max}^k} \tag{3}$$

where Δ_i^k is the absolute difference between the maximum and the sequence value of MRR. $\Delta_{\min}^k$ and $\Delta_{\max}^k$, are the lowest and highest values of Δ_i^k, λ is the distinguishing coefficient (taken as 0.5), k is quality characteristics and i is the experiments number. The GRCs calculated for MRR and WOC are given in Table 6.

Further, the Grey relational grades (GRG) corresponding to the trial conditions (Table 4) were calculated by averaging the GRCs for each response parameter as follows:

Table 6. Normalized values of response parameters, GRCs and GRGs for MRR and WOC.

Number	Normalized response parameters		GRC		GRG	
	MRR	WOC	MRR	WOC	Value	Order
1	0.0000	1.0000	0.3333	1.0000	0.6667	4
2	0.4954	0.8941	0.4977	0.8252	0.6615	7
3	0.9174	0.8294	0.8583	0.7456	0.8019	1
4	0.3486	0.9814	0.4343	0.9642	0.6992	2
5	0.8544	0.6048	0.7744	0.5585	0.6665	6
6	0.6984	0.3595	0.6237	0.4384	0.5311	9
7	0.9117	0.5459	0.8499	0.5241	0.6870	3
8	0.7053	0.3975	0.6291	0.4535	0.5413	8
9	1.0000	0.0000	1.0000	0.3333	0.6667	5

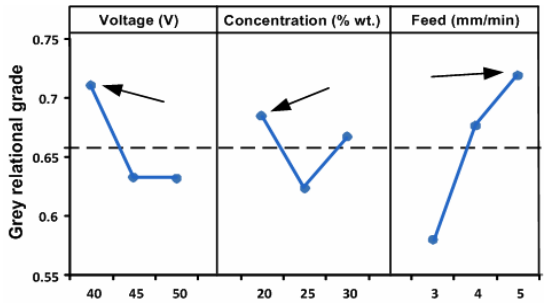

Fig. 5. GRG plot.

$$\gamma_i = \frac{1}{n}\sum_{k=1}^{n}\xi_i^k \tag{4}$$

where n is the number of response parameters and k is the response parameter number. For the present study, the above equation can be written as follows:

$$\gamma_i = \frac{1}{2}\left(\xi_i^{mrr} + \xi_i^{woc}\right). \tag{5}$$

The GRGs calculated using the above relation are shown in Table 6. The higher order GRG indicates that the experimental result correspond to higher grade is nearer to the ideal quality characteristic. Therefore, combination of optimal control parameter can be obtained from the analysis of GRG. For the present analysis, the highest relational grade was obtained corresponding to the trial condition number 3, i.e. A1B3C3 (40 V-30 wt% -5 mm/min).

However, it is required to consider each control parameter effect on the GRG at all levels because of the orthogonal design of experiments. The GRG mean and the total mean for each control parameter are shown in Table 7. It is to be noted that the feed rate, applied voltage and concentration of electrolyte are now ranked 1, 2 and 3, respectively. This highlights the fusion of the information corresponding to the responses - MRR and WOC as these ranks (delta values) were computed using data for both the responses. Thus, the revised order of

Table 7. Mean GRG and significance rank.

Level	Mean GRG		
	Voltage	Electrolyte concentration	Feed rate
1	0.7100	0.6842	0.5796
2	0.6322	0.6230	0.6757
3	0.6316	0.6665	0.7184
Delta	0.0784	0.0612	0.1388
Rank	2	3	1

ranks may be considered as the result of the net effect of the control parameters on the performance of the process. Fig. 5 shows the graphical representation of GRGs. The combination for optimal control parameter can be determined from the Fig. 4 as A1B1C3 i.e., applied voltage (level 1): 40 V, electrolyte concentration (level 1): 20 wt%, and feed rate (level 3): 5 mm/min. The result indicates the optimal machining performance while simultaneously considering both the contradicting quality characteristics (in the present case). It is known that the chemical etching action has the least effect on the material removal in ECDM while the applied voltage has significant influence on the sparking and hence in MRR. However, higher applied voltage tends to cause more overcut (hence, higher WOC) while higher feed rate takes the spark source away from the already machined zone at a faster rate, leaving less time to cause further overcut. Thus, this approach considers the accuracy factor (WOC, here) to a reasonable extent while determining the optimal processing condition and indicating the process performance.

5.3 Analysis of variance (ANOVA)

The main objective of ANOVA is to find out the relative importance of control parameters on the multiple quality characteristics and was carried for GRA analyses. The results of ANOVA of GRGs are shown in Table 8. The analysis indicates that the most influential parameter was the feed rate with the contribution of 56.97 %, followed by applied voltage and concentration of the electrolyte with the contribution of 22.91 % and 11.18 %, respectively. This observation is in agreement with the ranks of the parameters as illustrated in Table 7.

5.4 Confirmation test

It is necessary to verify the improvements in the response parameters through confirmation tests after obtaining the combination of optimal control parameter. The estimated GRG for the combination of optimal control parameter can be calculated using the following expression.

$$\eta = \eta_g + \sum_{i=1}^{p}\left(\eta_m - \eta_g\right) \tag{6}$$

Table 8. ANOVA analysis results for GRGs.

Factors	Sum of squares	DOF	Variance	F-ratio	Contribution (%)
Voltage	0.0122	2	0.0061	2.5607	22.91
Electrolyte concentration	0.0059	2	0.0029	1.2496	11.18
Feed rate	0.0303	2	0.0151	6.3686	56.97
Error	0.0047	2	0.0023		
Total	0.0531	8			

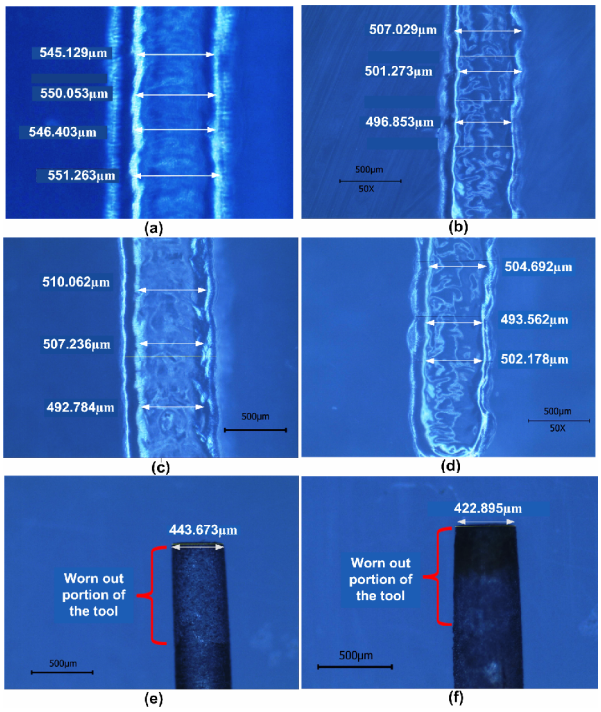

Fig. 6. Width of machined channel on quartz glass: (a) Result of average condition; (b)-(d) results of confirmatory machining with optimal condition obtained from the GRA; (e), (f) worn out portion of the tool-electrodes used for confirmation tests.

where η_g is the GRG grand mean, η_m is the mean of GRG for a control parameter, and p is the number of control parameters.

The estimated GRG for the combination of optimal control parameters (A1B1C3) established by GRA was 0.7968. Table 9 shows the confirmation test results conducted based on the optimal control parameters. The results of three confirmation tests reveal that the MRR was increased from an average condition (0.4053 mm^3/min) to optimal condition (0.4166 mm^3/min i.e. an average of 0.3968 mm^3/min, 0.432 mm^3/min and 0.421 mm^3/min in the first, second and third test, respectively) as obtained through GRA. Fig. 6 shows the improvement in the WOC form average condition (0.0982 mm) to optimal condition (0.0517 mm, i.e. an average of 0.0517, 0.0533 and 0.0501 mm in the first, second and third confirmation tests, respectively) and the worn out portion of the tool-electrode used for confirmation test (Fig. 6(d)). The observed

Table 9. Comparison of results of the confirmation experiments with the results of the experiments conducted at average levels.

	Machining condition at average levels	Optimal control parameters			
		A1B1C3			
Level combination	A2B2C2	Experimental			Average
MRR (mm^3/min)	0.4053	0.3968	0.432	0.421	0.4166
WOC (mm)	0.0982 (Fig. 6(a))	0.0517 (Fig. 6(b))	0.0533 (Fig. 6(c))	0.0501 (Fig. 6(d))	0.0515
GRG	0.6749	0.7561	0.7858	0.7677	

channel widths were obtained within the same range in all cases, which indicate consistency in the results obtained. The analysis of tool wear was not considered in current communication. However, it is clear that, the multiple quality characteristics - MRR and WOC in the ECDM process can be simultaneously improved (Fig. 6 and Table 9) by determining the optimal parametric condition through the GRA approach.

6. Conclusions

In this paper, the benefit of GRA over S/N ratio analysis has been highlighted in the machining of micro-channels on quartz glass. Taguchi's design with GRA analysis was used to establish the combination of optimal control parameter for the multiple response parameters (MRR and WOC). The following major conclusions are drawn from the present investigation:

(1) The S/N ratio analysis could be used as an initial process monitoring parameter. The S/N ratio analysis could yield different optimal conditions for different responses (here: A3B3C3 with respect to MRR, i.e. applied voltage of 50 V, concentration of electrolyte of 30 wt%, and feed rate of 5 mm/min; while A1B1C2 for the response WOC, i.e. applied voltage of 40V, concentration of electrolyte of 20 wt%, and feed rate of 4 mm/min).

(2) The GRA converts the multi objective optimization into single objective optimization problems based on GRGs. Thus, the optimal control parameters (A1B1C3) were obtained by integrating into a combined effect for higher MRR and lower WOC, such as the applied voltage of 40 V (level 1), concentration of electrolyte of 20 wt% (level 1), and feed rate of 5 mm/min (level 3) with the contribution of 22.91 %, 11.18 % and 56.97 %, respectively.

(3) The most dominant factor for micro-channel machining of quartz glass was the feed rate when compared to applied voltage and electrolyte concentration.

References

[1] B. K. Bhuyan and V. Yadava, Experimental modeling and multi-objective optimization of traveling wire electrochemical spark machining (TW-ECSM) process, *Journal of Me-*

chanical Science and Technology, 27 (8) (2013) 2467-2476.
[2] C. P. Cheng, K. L. Wu, C. C. Mai, C. K. Yang, Y. S. Hsu and B. H. Yan, Study of gas film quality in electrochemical discharge machining, *International Journal of Machine Tools & Manufacture*, 50 (2010) 689-697.
[3] Z. P. Zheng, W. H. Cheng, F. Y. Huang and B. H. Yan, 3D Microstructuring of pyrex glass using the electrochemical discharge machining process, *Journal of Micromechanics and Microengineerin*g, 17 (2007) 960-966.
[4] M. Goud, A. K. Sharma and C. Jawalkar, A review on material removal mechanism in electrochemical discharge machining (ECDM) and possibilities to enhance the material removal rate, *Precision Engineering,* 45 (2016) 1-17.
[5] M. S. Han, B. K. Min and S. J. Lee, Micro-electrochemical discharge cutting of glass using a surface-textured tool, *CIRP Journal of Manufacturing Science and Technology*, 4 (2011) 362-369.
[6] X. D. Cao, B. H. Kim and C. N. Chu, Micro structuring of glass with features less than 100μm by electrochemical discharge machining, *Precision Engineering*, 33 (2009) 459-465.
[7] J. H. Jung and W. T. Kwon, Optimization of EDM process for multiple performance characteristics using Taguchi method and Grey relational analysis, *Journal of Mechanical Science and Technology*, 24 (5) (2010) 1083-1090.
[8] R. Adalarasan, M. Santhanakumar and A. S. Sundaram, Optimization of weld characteristics of friction welded AA 6061-AA 6351 joints using grey-principal component analysis (G-PCA), *Journal of Mechanical Science and Technology*, 28 (1) (2014) 301-307.
[9] J. K. Kim, Experimental study on the optimum design of the flow-path system for a low noise indoor package air-conditioner, *Journal of Mechanical Science and Technology*, 28 (4) (2014) 1277-1283.
[10] P. Lijo and S. S. Hiremath, Characterization of microchannels in electrochemical discharge machining process, *Applied Mechanics and Materials*, 490 (2014) 238-242.
[11] C. S. Jawalkar, A. K. Sharma and P. Kumar, Investigations on performance of ECDM process using NaOH and $NaNO_3$ electrolytes while micro machining soda lime glass, *International Journal Manufacturing Technology and Management*, 28 (2014) 80-93.
[12] P. K. Gupta, A. Dvivedi and P. Kumar, Developments on electrochemical discharge machining: A review of experimental investigations on tool electrode process parameters, *Proc. of the Institution of Mechanical Engineers, Part B: Journal of Engineering Manufacture* (2014) 1-11.
[13] C. T. Yang, S. L. Song, B. H. Yan and F. Y. Huang, Improving machining performance of wire electrochemical discharge machining by adding SiC abrasive to electrolyte, *International Journal of Machine Tools & Manufacture*, 46 (2006) 2044-2050.
[14] X. D. Cao, B. H. Kim and C. N. Chu, Hybrid micromachining of glass using ECDM and micro grinding, *International Journal of Precision Engineering and Manufacturing*, 14 (2013) 5-10.
[15] W. Feng and L. Hua, Multi-objective optimization of process parameters for the helical gear precision forging by using Taguchi method, *Journal of Mechanical Science and Technology,* 25 (6) (2011) 1519-1527.
[16] *http://www.machsupport.com/software/mach3/* (as accessed on May 25th 2015).
[17] S. V. Kumar and M. P. Kumar, Optimization of cryogenic cooled EDM process parameters using grey relational analysis, *Journal of Mechanical Science and Technology*, 28 (9) (2014) 3777-3784.
[18] K. Shi, D. Zhang and J. Ren, Optimization of process parameters for surface roughness and microhardness in dry milling of magnesium alloy using Taguchi with grey relational analysis, *International Journal of Advanced Manufacturing Technology*, 81 (2015) 645-651.

Mudimallana Goud is pursuing his Ph.D. in the Department of Mechanical and Industrial Engineering at Indian Institute of Technology Roorkee, Roorkee, India.

Apurbba Kumar Sharma is an Associate Professor in the Department of Mechanical and Industrial Engineering at the Indian Institute of Technology Roorkee, India. Presently, he is also Associate Dean, Academic Studies. He has supervised ten doctoral programs and completed four externally funded research projects. He has published nearly ninety research articles in reputed journals and filed six patents in India. He has chaired several technical sessions in international conferences. His prime research interests include - advanced manufacturing processes, micro machining, fine finishing, and microwave material processing. Dr. Sharma is a DAAD fellow, and Fellow of Institution of Engineers (India).